

Resistance Against Ricin-Induced Apoptosis in a Brefeldin A-Resistant Mutant Cell Line (BER-40) of Vero Cells

Tadashi Tamura, Tatsuya Oda,¹ and Tsuyoshi Muramatsu

Division of Biochemistry, Faculty of Fisheries, Nagasaki University, Bunkyo-machi, Nagasaki, 852-8521

Received May 11, 2002; accepted July 2, 2002

We have found that a brefeldin A (BFA)-resistant mutant cell line derived from Vero cells (BER-40) is highly resistant to ricin-induced apoptosis as compared with parental Vero cells. In BER-40 cells, all apoptotic events caused by ricin including cytolysis, nuclear morphological changes, and DNA fragmentation occur to a lesser extent than in Vero cells, even though both cell lines show similar sensitivities to ricin-mediated inhibition of protein synthesis. Furthermore, no significant apoptotic signaling events, such as increases in caspase-3 and -9-like activities, release of cytochrome *c* from mitochondria, or the cleavage of PARP, were observed in BER-40 cells under the conditions at which these changes were evident in Vero cells. Intracellular biochemical changes associated with ricin-induced apoptosis, such as the depletion of glutathione and an increase in free Zn²⁺, were also less apparent in BER-40 cells than in Vero cells. BER-40 cells were also found to be highly resistant to apoptosis induced by other toxins with different intoxication mechanisms such as diphtheria toxin, modeccin, and anisomycin. These results suggest that the entire apoptotic signal transduction mechanism in BER-40 cells, which may be triggered after the inhibition of protein synthesis by toxins, becomes resistant. Since MDCK cells, a naturally BFA resistant cell line, are highly sensitive to ricin-induced apoptosis, it seems likely that the BFA resistance phenotype may not necessarily lead to resistance to apoptotic cell death. Probably the underlying BFA-resistance mechanism in BER-40 cells is distinct from that in MDCK cells, and the resistance to ricin-induced apoptosis of BER-40 cells may be a unique phenotype acquired concomitantly with BFA-resistance.

Key words: apoptosis, brefeldin A, ricin, the Golgi complex.

Ricin, a plant protein toxin (66 kDa) present in castor beans, consists of two structurally and functionally different subunits (A and B) linked together through a single disulfide bond. The A subunit (32 kDa) inactivates ribosomes by enzymatically removing a specific adenine residue from the 28S RNA of the 60S ribosomal subunit, leading to the inhibition of cellular protein synthesis. The B subunit binds to cell surface carbohydrates containing galactose or *N*-acetylgalactosamine residues (1–3).

It has been demonstrated that ricin is transported to the Golgi apparatus, mainly to the *trans*-Golgi network, during intoxication (4, 5). Youle and Colombatti (6) have shown that a hybridoma cell secreting antibodies against ricin is resistant to the toxic effects of ricin, suggesting an intersection of the endocytic and exocytic pathways in target cells during the intoxication process. The Golgi apparatus is known to play a central role in regulating the sorting and trafficking of proteins through the exocytic and endocytic

pathways (7, 8). Brefeldin A (BFA), a lipophilic fungal antibiotic, has been shown to affect the structure and function of the Golgi apparatus, including the inhibition of protein transport from the endoplasmic reticulum (ER) to the Golgi complex (9, 10), the rapid and reversible disassembly of the Golgi complex (11, 12), and the retrograde transport of resident and itinerant Golgi proteins to the ER (12, 13). Yoshida *et al.* (14, 15) have shown that BFA blocks the intoxication of Vero and other cell lines by ricin and other protein toxins such as modeccin and *Pseudomonas* toxin, but has no effect on the cytotoxicity of diphtheria toxin. Thus, it has been speculated that the Golgi apparatus is involved in the intoxication process of these protein toxins other than diphtheria toxin. On the other hand, a BFA-resistant mutant cell line of Vero cells (BER-40) (16) and naturally BFA-resistant cell lines, MDCK and PtK₁ cells, are not protected by BFA against ricin cytotoxicity and the Golgi apparatus of these cell lines are BFA-resistant (16–20).

Recent studies have demonstrated that ricin induces cell lysis and DNA fragmentation in a process reminiscent of programmed cell death or apoptosis (21–23), although the detailed mechanism is still unclear. In the present study, we investigated the apoptotic cytotoxicity of ricin in Vero and BER-40, and found that BER-40 cells are highly resistant to ricin-induced apoptosis as judged by nuclear morphological changes, DNA fragmentation, cytolysis, and several other intracellular changes including apoptotic signaling events.

¹To whom correspondence should be addressed. Tel: +81-95-847-1111, Fax: +81-958-44-3516, E-mail: t-oda@net.nagasaki-u.ac.jp

Abbreviations: BFA, brefeldin A; MCA, 4-methyl-coumaryl-7-amide; MDCK, Madin-Darby canine kidney; PBS, phosphate-buffered saline; BSA, bovine serum albumin; PARP, poly(ADP-ribose)polymerase; LDH, lactate dehydrogenase; DAEC, dansylaminoethyl-cyclen; PMSF, phenylmethylsulfonyl fluoride; CHAPS, 3-[(3-cholamidopropyl)dimethylammonio]-1-propanesulfonic acid.

MATERIALS AND METHODS

Materials—Ricin was isolated from small castor beans as described by Mise *et al.* (24). Diphtheria toxin was purchased from Swiss Serum and the Vaccine Institute (Berne, Switzerland). Modeccin was obtained from Inland Laboratories (Austin, TX). Brefeldin A (BFA) was purchased from Pierce (Rockford, IL). H33258 (Hoechst 33258) was purchased from Wako Chem. (Tokyo). The caspase family protease inhibitor (Z-Asp-CH₂-DCB) and fluorescent tetrapeptide substrates of caspases (Ac-DEVD-MCA for caspase-3, Ac-VEID-MCA for caspase-6, and Ac-LEHD-MCA for caspase-9) were obtained from the Peptide Institute (Osaka). [³H]Leucine (60 Ci/mmol) was obtained from NEN Research Products (Boston, MA). Dansylaminoethyl-cyclen (DAEC), a Zn²⁺ specific fluorescent probe, was purchased from Dojin Chemical Laboratories, Kumamoto, Japan.

Cell Culture—Vero (African green monkey kidney) and MDCK (Madin-Darby canine kidney) cells were from the American Type Culture Collection (Rockville, MD). The BFA-resistant mutant cell line, BER-40, was isolated from Vero cells following ethylmethanesulfonate mutagenesis (16). These cell lines were grown as monolayers in α -minimal essential medium (α -MEM) supplemented with 10% fetal bovine serum, 10 μ g each of adenosine, guanosine, cytidine, and thymidine per ml of medium, penicillin (100 μ g/ml) and streptomycin (100 μ g/ml) as described previously (25). The cells were subcultured 1 day before use by treatment with 0.1% trypsin–0.05% EDTA in phosphate-buffered saline (PBS).

Cytotoxicities of BFA and Various Anticancer Agents—The cytotoxicities of BFA and various anticancer agents were measured by the inhibition of colony formation. An appropriate number of cells (200–250 cells per well in a 24-well plate) were cultured with varying concentrations of each agent in growth medium for 6 days. The number of colonies formed was counted after staining with 1% methylene blue in 50% methanol. Clusters of 40 or more cells were considered to be colonies.

Measurement of Protein Synthesis Inhibition—Cells were inoculated at a density of 5×10^4 cells/well in 0.2 ml of medium using 48-well plates. One day later, varying concentrations of ricin or other toxins were added to the cells and the cells were incubated for 3 h in serum-free α -MEM containing 35 μ M BSA at 37°C. After removal of the medium, the cells were incubated with 1 μ Ci/ml of [³H]leucine for 45 min at 37°C in leucine-free medium. The incorporation of [³H]leucine into the perchloric acid/phosphotungstic acid-insoluble materials was determined as described previously (25). In the case of anisomycin, the rate of incorporation of [³H]leucine into the acid-insoluble materials was measured in the presence of the indicated concentrations of anisomycin. The results are expressed as the percentage of incorporation in control cells incubated without toxin but otherwise treated in the same way.

Cytolytic Assay—The cytolytic activities of toxins were measured by the lactate dehydrogenase (LDH) release assay in which LDH released from lysed cells was determined by measuring the reduction of 2-(*p*-iodophenyl)-3-(*p*-nitrophenyl)-5-phenyltetrazolium chloride as described previously (26). In brief, 2×10^4 cells/well in a 96-well plate in α -MEM containing 35 μ M BSA were incubated with varying

concentrations of ricin or other toxins for 18 h at 37°C. The plates were then centrifuged (1,500 $\times g$, 10 min), and the supernatant (50 μ l) in each well was subjected to LDH assay.

DNA Fragmentation Assay—Varying concentrations of ricin or other toxin were added cell monolayers in dishes (35 mm) (6×10^5 cells/dish) in α -MEM containing 35 μ M BSA, and the cells were incubated for the indicated periods of time at 37°C. Then the cells were washed once with PBS and lysed in 1 ml of ice-cold lysis buffer (0.5% Triton X-100, 10 μ M Tris-HCl, pH 8.0, 20 mM EDTA). The lysates were subsequently centrifuged for 30 min at 13,000 $\times g$ to separate DNA fragments (supernatant) from intact DNA (pellet). The DNA contents of the supernatant and pellet fractions were determined using diphenylamine reagent as described previously (26).

Nuclear Staining—Cells grown on glass coverslips were incubated with the indicated concentrations of ricin in α -MEM containing 35 μ M BSA for 18 h at 37°C. The cells were washed with PBS, subsequently fixed with 1% glutaraldehyde for 30 min at room temperature, and then stained with Hoechst 33258 (40 μ M) for 5 min at room temperature. The cells were then observed under an Olympus BX-60 fluorescence microscope.

Detection of Cytosolic Cytochrome *c*—Cell monolayers in dishes (100 μ m) (5×10^6 cells/dish) in α -MEM containing 35 μ M BSA were incubated with 10 ng/ml of ricin for the indicated periods of time at 37°C. The cells were washed twice with PBS, scraped off, and pelleted by centrifugation. The pelleted cells were resuspended in 100 μ l of ice-cold extraction buffer containing 250 mM sucrose, 50 mM Tris-HCl, 1 mM EGTA, 1 mM DTT, 1 mM 1,10-phenanthroline, 0.1 mM PMSF, pH 7.4, and then homogenized by passing the suspension 10 times up and down through a 1 ml blue tip on a pipette and then 10 times through a 1 ml syringe with a 22G1 1/4 needle. Following centrifugation (21,000 $\times g$ for 10 min at 4°C), the extract was mixed with SDS-sample buffer and boiled for 5 min. Samples containing 50 μ g of protein were subjected to SDS-PAGE in a 5–20% gradient polyacrylamide gel. The protein was then transferred to a PVDF membrane. Western blotting using an anti-cytochrome *c* rabbit polyclonal antibody (Santa Cruz) and a chemiluminescence system was used to detect antigen-antibody complexes on the PVDF membrane as previously described (26).

Peptide Cleavage Assay—Cell monolayers in dishes (35 mm) (6×10^5 cells/dish) in α -MEM containing 35 μ M BSA were incubated with 10 ng/ml ricin for the indicated periods of time at 37°C. Then the cells were washed once with PBS and suspended in 200 μ l of ice-cold extraction buffer (10 μ M HEPES/KOH buffer, pH 7.4, 2 mM EDTA, 0.1% CHAPS, 5 mM DTT, 1 mM PMSF) as described (29). After repeated freezing and thawing, cell debris was removed by centrifugation at 13,000 $\times g$ at 4°C for 20 min. The supernatants were incubated with 10 μ M fluorescent substrate at 37°C for 10 min, and then peptide cleavage was analyzed at an excitation wavelength of 380 nm and an emission wavelength of 460 nm as previously described (29).

Detection of PARP Cleavage—Ricin-treated and -untreated cells (60 mm diameter) (2×10^6 cells/dish) were lysed in RIPA buffer (10 μ M Tris-HCl, pH 7.4, 150 mM NaCl, 5 mM EDTA, pH 7.4, 1% Triton X-100, 0.1% SDS, 0.1 mM *N*-tosyl-L-lysine chloromethyl ketone, 0.2 mM *N*-tosyl-L-phe-

nylalanine chloromethyl ketone, 0.5 mM phenylmethylsulfonyl fluoride, 2 $\mu\text{g/ml}$ aprotinin, 0.5 $\mu\text{g/ml}$ leupeptin, and 1 μM pepstatin). Twenty micrograms of protein per lane was subjected to SDS-PAGE analysis, followed by transfer to a PVDF membrane and hybridization with anti-PARP rabbit polyclonal antibody as previously reported (26). Protein bands were visualized with biotin-conjugated goat anti-rabbit immunoglobulin G using a chemiluminescence system as previously described (26).

Immunoblot Analysis of Bcl-2—Cell monolayers in dishes (60 mm) (2×10^6 cells/dish) in α -MEM containing 35 μM BSA were washed twice with PBS, scraped off, and pelleted by centrifugation. The pelleted cells were resuspended in 100 μl of extraction buffer (10 μM HEPES, 150 mM NaCl, 1 mM EGTA, 1% CHAPS, 1 mM phenylmethylsulfonyl fluoride, 10 μM aprotinin, 10 μM leupeptin, 10 μM pepstatin, pH 7.4), and then sonicated for 2 min at 4°C. Following centrifugation (21,000 $\times g$ for 10 min at 4°C), the extract was mixed with SDS-sample buffer and boiled for 5 min. Samples containing 50 μg of protein were subjected to SDS-PAGE in a 5–20% gradient polyacrylamide gel. The protein was then transferred to a PVDF membrane. Western blotting using an anti-Bcl-2 mouse monoclonal antibody (Boehringer Mannheim) and suitable peroxidase-conjugated secondary antibodies (Amersham Pharmacia Biotech) was performed as described above.

Distribution of Probe-Stainable Zn²⁺—Cells grown on glass coverslips were incubated with or without 10 ng/ml of ricin in α -MEM containing 35 μM BSA for 18 h at 37°C. To visualize intracellular DAEC-sensitive Zn²⁺, DAEC (final 10 μM) was added to the cells and the cells were incubated for 10 min at 37°C. After washing with PBS, the cells were observed under a fluorescence microscope.

Measurement of Glutathione—The intracellular glutathione content was determined by the recycling assay based on the reduction of 5,5-dithiobis (2-nitrobenzoic acid) with glutathione reductase and NADPH (27). Sample preparation and assay procedures are described elsewhere (28).

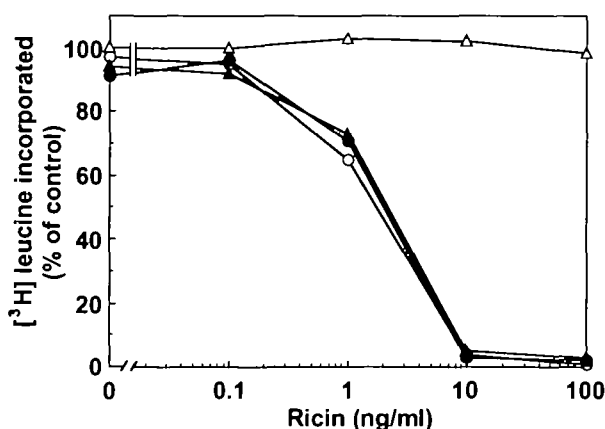


Fig. 1. Effect of BFA on the protein synthesis inhibitory activity of ricin in Vero and BER-40 cells. Vero (○, △) or BER-40 cells (●, ▲) grown in 48-well plates (5×10^4 cells/well) were preincubated in α -MEM containing 35 μM BSA with (△, ▲) or without (○, ●) 0.1 $\mu\text{g/ml}$ BFA for 1 h at 37°C, followed by the addition of varying concentrations of ricin. Cells were incubated for another 3 h in the presence or absence of BFA, and then labeled with [³H]leucine for 45 min in leucine-free medium for the measurement of protein synthesis. Each point represents the average of duplicate measurements.

RESULTS

Cytotoxic Effects of BFA and Various Anticancer Agents on Vero and BER-40 Cells—As shown in Table I, the IC_{50} of BFA on BER-40 cells was about 40-fold higher than that on Vero cells. These results indicate that the BFA-resistant phenotype was maintained stably during serial cell culture in the absence of BFA for more than 10 years. In contrast to the resistance to BFA cytotoxicity, BER-40 cells showed no significant resistance to various anticancer agents that are usually affected by the multidrug resistance gene product via active efflux.

Effect of BFA on Ricin-Mediated Protein Synthesis Inhibition in Vero and BER-40 Cells—It has been shown that disruption of the Golgi complex by BFA results in the inhibition of the protein synthesis inhibitory activity of ricin and other protein toxins (14, 15). As shown in Fig. 1, pretreatment with 0.1 $\mu\text{g/ml}$ BFA protected Vero cells but not BER-40 cells from ricin-mediated protein synthesis inhibition. Thus it appears that the BFA-resistance phenotype of BER-40 cells is also confirmed in the lack of a protective effect of BFA against ricin toxicity. On the other hand, Vero and BER-40 cells showed similar sensitivities to ricin-mediated protein synthesis.

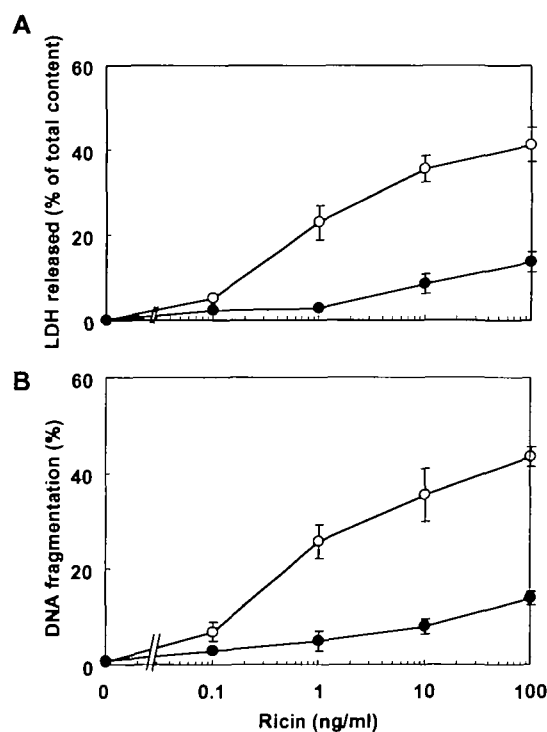


Fig. 2. Ricin-induced cytolysis (A) and DNA fragmentation (B) in Vero and BER-40 cells. (A) Vero (○) or BER-40 (●) cells in 96-well plates (2×10^4 cells/well) were treated with varying concentrations of ricin in α -MEM containing 35 μM BSA for 18 h at 37°C. The supernatant of each well was then subjected to the LDH assay as described under "MATERIALS AND METHODS." (B) Vero (○) or BER-40 (●) cells (6×10^5 cells/dish) (35 mm) were incubated with varying concentrations of ricin in α -MEM containing 35 μM BSA for 18 h at 37°C. DNA fragmentation in the ricin-treated cells was assayed with diphenylamine as described under "MATERIALS AND METHODS." Each point represents the average of duplicate measurements.

Comparison of Ricin-Induced Apoptotic Events between Vero and BER-40 Cells—As described above (Fig. 1), Vero and BER-40 cells showed almost the same sensitivity to ricin-mediated protein synthesis inhibition. After prolonged incubation, DNA fragmentation and subsequent cytolysis were induced by ricin in Vero cells at doses in a similar concentration range as cause the inhibition of protein synthesis (Fig. 2). However, BER-40 cells were highly resistant to ricin-induced apoptosis as seen to a lesser extent for DNA

fragmentation and eventual cytolysis. After 18 h exposure to 10 ng/ml ricin, a large proportion of adherent Vero cells detached from the plates and the remaining cells showed apoptotic nuclear morphological changes (Fig. 3B). In contrast to Vero cells, no such morphological changes were observed in BER-40 cells after treatment with ricin (Fig. 3).

Release of Mitochondrial Cytochrome *c* and the Subsequent Activation of Caspase-9-Like Activity in Ricin-Treated Vero and BER-40 Cells—It is known that cytochrome *c* is released from mitochondria during apoptosis, and that cytosolic cytochrome *c* activates caspase-9 together with Apaf-1, leading to caspase-dependent apoptotic cell death (30). We investigated the release of cytochrome *c* from mitochondria in ricin-treated Vero and BER-40 cells by protein immunoblot analysis. As shown in Fig. 4, a gradual increase in the cytosolic cytochrome *c* level concomitant with an increase in caspase-9-like activity was observed in ricin-treated Vero cells, whereas neither a detectable increase in the cytochrome *c* level in cytosol nor a marked activation of caspase-9-like activity was observed in BER-40 cells.

Caspase-3-Like Activity and PARP Cleavage in Ricin-Treated Vero and BER-40 Cells—It has been shown that in many apoptotic systems activated caspase-9, through a cooperation with cytochrome *c* and Apaf-1, activates caspase-3, which in turn cleaves cytosolic and nuclear target molecules such as PARP. Consistent with these findings, the caspase-3-like activity in Vero cells increased gradually by more than 10-fold after 18 h of incubation with 10 ng/ml

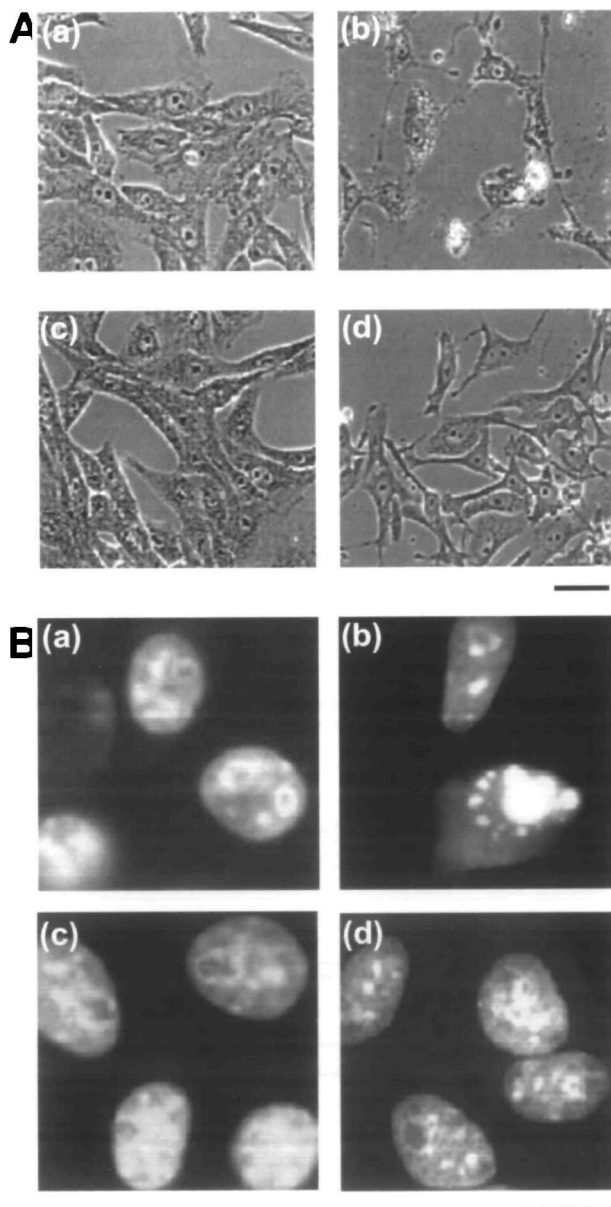


Fig. 3. Effect of ricin on cellular (A) and nuclear morphology (B) in Vero and BER-40 cells. (A) Vero (a, b) or BER-40 (c, d) cells grown on coverslips were incubated with (b, d) or without (a, c) 10 ng/ml ricin in α -MEM containing 35 μ M BSA for 18 h at 37°C, and then observed under a phase contrast microscope. (B) Vero (a, b) or BER-40 (c, d) cells grown on coverslips were incubated with (b, d) or without (a, c) 10 ng/ml ricin in α -MEM containing 35 μ M BSA for 18 h at 37°C. The treated cells were fixed and stained with Hoechst 33258 (40 μ M) for 10 min, and observed under a fluorescence microscope. The bars indicate 20 μ m.

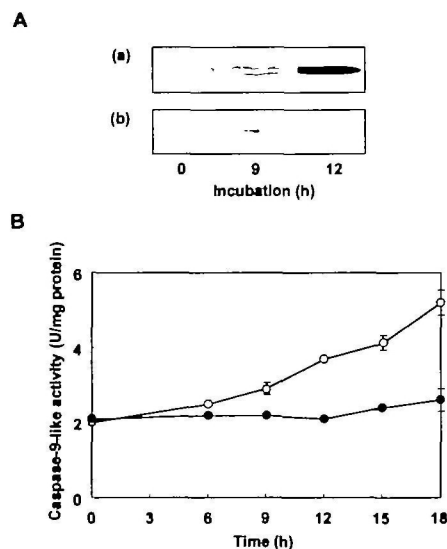


Fig. 4. Time course analysis of cytosolic cytochrome *c* levels (A) and caspase-9-like activities (B) in ricin-treated Vero or BER-40 cells. (A) Vero (a) or BER-40 (b) cells (5×10^6 cells/dish) (100 mm) in α -MEM containing 35 μ M BSA were treated with 10 ng/ml ricin for the indicated periods of time (0, 9, 12 h) at 37°C, and then cytosolic extracts were prepared for immunoblotting analysis with anti-cytochrome *c* antibody as described under "MATERIALS AND METHODS." (B) Vero (○) or BER-40 (●) cells (6×10^6 cells/dish) (35 mm) in α -MEM containing 35 μ M BSA were treated with 10 ng/ml ricin for the indicated periods of time at 37°C, and then cytosolic extracts were prepared from the treated cells. Caspase-9-like activities in each extract were determined using the fluorescent substrate as described under "MATERIALS AND METHODS." Each point represents the average of duplicate measurements.

ricin as compared to the 0 time value (Fig. 5). In contrast to Vero cells, only a slight increase in caspase-3-like activity was observed in BER-40 cells. Furthermore, immunoblot analysis using an anti-PARP antibody, which recognizes both the parental PARP (113 kDa) and its cleavage product (89 kDa), revealed that a substantial amount of PARP was cleaved in Vero cells after 18 h incubation with ricin, while there was no detectable cleavage fragment in lysates prepared from ricin-treated BER-40 cells (Fig. 5B).

Bcl-2 Levels in Ricin-Treated Vero and BER-40 Cells—Bcl-2 is known to play a prominent role in regulating apoptosis and enhancing cell survival in response to a wide variety of apoptotic stimuli (31). Bcl-2 acts primarily to pre-

serve mitochondrial integrity and suppress the release of cytochrome *c* (32). In fact, gene transfer studies have shown that elevated levels of Bcl-2 can block or delay apoptotic cell death induced by certain apoptotic stimuli (33). To ascertain whether or not the increased resistance of BER-40 cells to ricin-induced apoptosis is due to an increase in the expression level of Bcl-2, we examined the levels of Bcl-2 in Vero and BER-40 cells during ricin treatment. As shown in Fig. 6, no significant differences in Bcl-2 levels were seen between Vero and BER-40 cells, and ricin did not affect the Bcl-2 expression level in either cell line.

Comparison of the Susceptibility of Vero and BER-40 Cells to Cytolysis Induced by Other Protein Synthesis Inhibitors—To examine whether BER-40 are resistant to other toxins that inhibit protein synthesis by different mechanisms, we tested the effects of diphtheria toxin, modeccin, and anisomycin on Vero and BER-40 cells. Both cell lines showed similar sensitivities to these toxins in terms of protein synthesis inhibition (data not shown). However, all of these toxins were less effective in BER-40 cells as compared to Vero cells in terms of the induction of cytolysis (Fig. 7).

Susceptibility of MDCK Cells to Ricin-Induced Apoptosis—To obtain insight into the relationship between BFA-resistance and resistance to ricin-mediated apoptosis, we examined the susceptibility of MDCK cells, which are naturally BFA-resistant cells, to ricin-induced apoptosis. As shown in Fig. 8, MDCK cells are even more sensitive to ricin-induced DNA fragmentation than Vero cells. In addition, typical apoptotic nuclear morphological changes were observed in ricin-treated MDCK cells as seen in Vero cells,

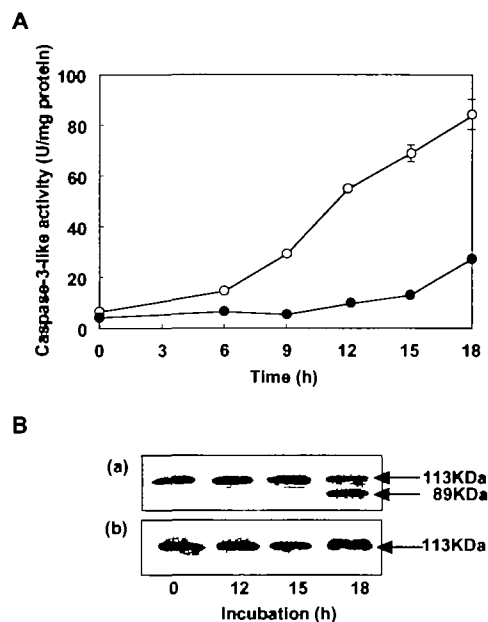


Fig. 5. Time course analysis of caspase-3-like activities (A) and PARP cleavage (B) in ricin-treated Vero or BER-40 cells. (A) Vero (○) or BER-40 (●) cells (6×10^6 cells/dish) (35 mm) in α -MEM containing 35 μ M BSA were treated with 10 ng/ml ricin for the indicated periods of time at 37°C, and then cytosolic extracts were prepared from the treated cells. Caspase-3-like activities in each extract were determined using the fluorescent substrate as described under "MATERIALS AND METHODS." (B) Vero (a) or BER-40 (b) cells (2×10^6 cells/dish) (60 mm) in α -MEM containing 35 μ M BSA were treated with 10 ng/ml ricin for the indicated periods of time (0, 12, 15, 18 h) at 37°C, and cell lysates were prepared for immunoblotting analysis with anti-PARP antibody as described under "MATERIALS AND METHODS."

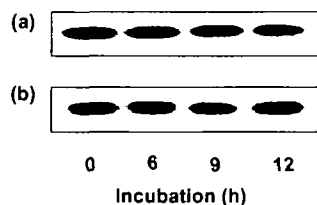


Fig. 6. Bcl-2 levels in ricin-treated Vero or BER-40 cells. Vero (a) or BER-40 (b) cells (2×10^6 cells/dish) (60 mm) in α -MEM containing 35 μ M BSA were treated with 10 ng/ml ricin for the indicated periods of time (0, 6, 9, 12 h) at 37°C, and cell lysates were prepared for immunoblotting analysis with anti-Bcl-2 antibody as described under "MATERIALS AND METHODS."

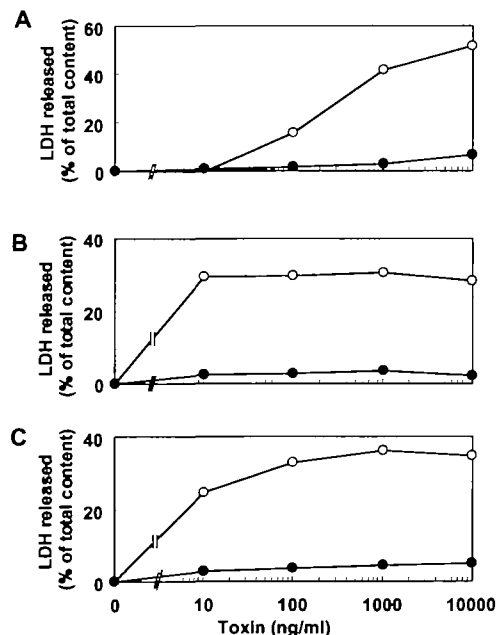


Fig. 7. Cytolysis induced by anisomycin (A), diphtheria toxin (B), and modeccin (C) in Vero and BER-40 cells. (A) Vero (○) or BER-40 (●) cells in 96-well plates (2×10^4 cells/well) were treated with varying concentrations of each toxin in α -MEM containing 35 μ M BSA for 18 h at 37°C, and then the supernatant from each well was subjected to LDH assay as described under "MATERIALS AND METHODS." Each point represents the average of duplicate measurements.

whereas no such changes are induced in BER-40 cells (Fig. 8B)

Other Biochemical Changes Accompanying Ricin-Induced Apoptosis in Vero and BER-40 Cells—We have previously reported that intracellular glutathione levels decrease gradually in U937 cells during ricin treatment (28). Since the depletion of glutathione is prevented by *N*-acetylcysteine, and this reducing reagent concomitantly protects U937 cells from ricin-induced apoptosis, intracellular glutathione levels may also reflect the progress of apoptosis. To verify further the differences between Vero and BER-40 cells, we measured intracellular glutathione levels in ricin-treated Vero and BER-40 cells. As shown in Fig. 9, glutathione depletion was delayed in BER-40 cells as compared with Vero cells. In addition to glutathione, our recent study suggested that an increase in intracellular free Zn^{2+} may take place during ricin-induced apoptosis (34). Thus, we investigated Zn^{2+} distribution in ricin-treated and untreated Vero and BER-40 cells *via* fluorescence microscopic observation with the Zn^{2+} -specific fluorescent probe, dancylaminoethyl-cyclen (DAEC). As shown in Fig. 10, more intense DAEC fluorescence dispersed throughout the entire

cytoplasm was observed in ricin-treated Vero cells, while there were only small amounts of fluorescence in the perinuclear region in ricin-treated BER-40 cells, indistinguishable from untreated control cells.

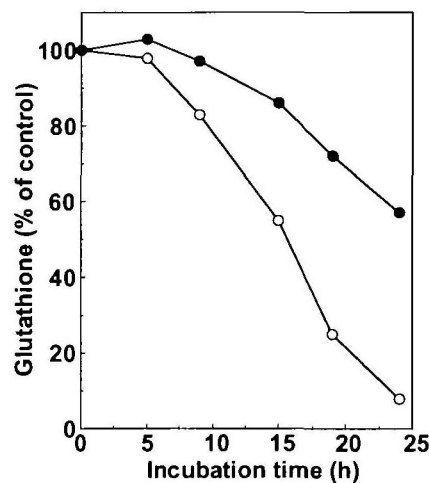


Fig. 9. Intracellular glutathione levels in ricin-treated Vero or BER-40 cells. Vero (○) or BER-40 (●) cells (6×10^6 cells/dish) (35 mm) were incubated with 10 ng/ml ricin in α -MEM containing 35 μ M BSA for the indicated periods of time at 37°C. Intracellular glutathione content in the ricin-treated cells was measured as described under "MATERIALS AND METHODS." Each point represents the average of duplicate measurements.

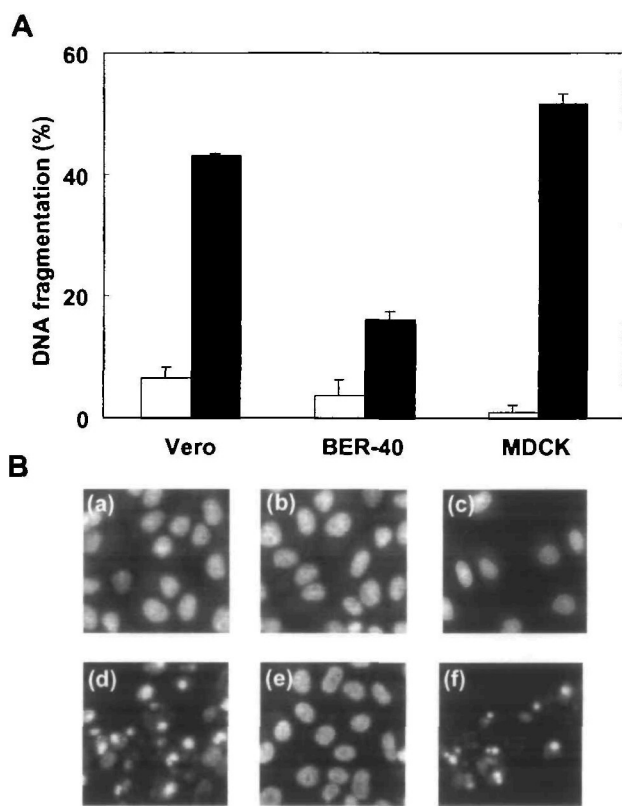


Fig. 8. Ricin-induced DNA fragmentation (A) and nuclear morphological changes (B) in Vero, BER-40, and MDCK cells. (A) Cells (6×10^6 cells/dish) (35 mm) were incubated with (■) or without (□) 10 ng/ml ricin in α -MEM containing 35 μ M BSA for 18 h at 37°C. DNA fragmentation in the treated cells was assayed with diphenylamine as described under "MATERIALS AND METHODS." (B) Vero (a, d), BER-40 (b, e), and MDCK cells (c, f) grown on coverslips were incubated with (d, e, f) or without (a, b, c) 10 ng/ml ricin in α -MEM containing 35 μ M BSA for 18 h at 37°C, and then nuclear morphological changes in the treated cells were observed as described in the legend to Fig. 3. The bar indicates 20 μ m.

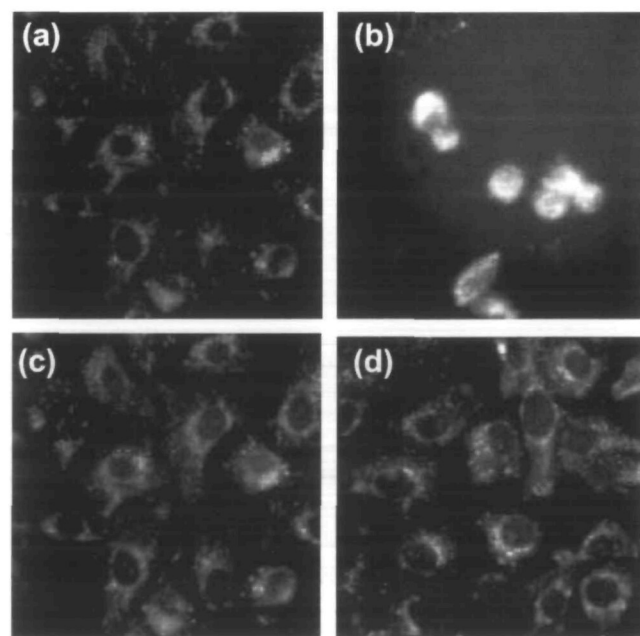


Fig. 10. Intracellular distribution of probe-stainable Zn^{2+} in ricin-treated and -untreated Vero or BER-40 cells. Vero (a, b) or BER-40 (c, d) cells grown on coverslips were incubated with (b, d) or without (a, c) 10 ng/ml ricin in α -MEM containing 35 μ M BSA for 18 h at 37°C. To visualize intracellular Zn^{2+} , dancylethylamino-cyclen (final 10 μ M) was added, and the cells were incubated for 10 min at 37°C. After washing with PBS, the cells were observed under a fluorescence microscope. The bar indicates 20 μ m.

DISCUSSION

BFA has been shown to produce a specific effect on the structural and functional integrity of the Golgi apparatus, resulting in the inhibition of protein secretion and a redistribution of the Golgi proteins into the endoplasmic reticulum (9–13). An early event in the action of BFA is the dissociation of the β -COP (110-kDa protein) from the Golgi membrane (35). Besides the effect of BFA on protein transport from the ER to the Golgi complex, BFA has been shown to affect transcytosis, and to alter vesicular transport between endosomes, lysosomes, and *trans*-Golgi networks (36, 37). In addition, the Golgi complexes in MDCK and PtK₁ cells have been found to be resistant to BFA in a genetically dominant fashion (37, 38). To gain insight into the mechanism by which BFA acts, a BFA-resistant mutant (BER-40) has been isolated from Vero cells (16). Although the detailed molecular mechanism of the BFA resistance in these cells remains to be elucidated, the resistance of these cells to BFA is reflected in several ways. The IC₅₀ of BFA as measured by the inhibition of colony formation is greatly increased in BER-40 cells as compared with parental Vero cells. The inhibition of protein secretion by BFA is reduced in BER-40 cells as compared with Vero cells. Unlike Vero cells, BER-40 cells are not protected by BFA from the cytotoxicities of ricin and other toxins (16). Furthermore, it has been shown that BFA induces little release of Golgi markers such as mannosidase II, NBD-ceramide, and β -COP from the Golgi region in BER-40 cells, whereas treatment of Vero cells with BFA results in a rapid release of these Golgi markers from the Golgi membrane to a more diffuse distribution in the cytosol (16). More importantly, it has been reported that the treatment of BER-40 cells with 2-deoxyglucose plus sodium azide, which are known to deplete cellular ATP/GTP levels and consequently lead to the dissociation of β -COP from the Golgi region (39), does not result in the release of β -COP from the Golgi membrane as found in Vero cells (16). These findings suggest that the mutation in BER-40 cells may alter the structure or assembly of the BFA-sensitive target(s) in such a way that the dynamic association of β -COP with the Golgi membrane is resistant to both BFA and ATP-depletion. These findings may also reduce the possibility of other drug-resistant mutations such as amplification of a multidrug-resistance gene or inactivation of BFA. This speculation is partly supported by the fact that the sensitivities of Vero and BEF-40 cells to a number of drugs that are usually affected by an amplification of the multidrug-resistance gene do not differ by very much (Table I).

In the present study we have found that BER-40 cells are highly resistant to ricin-induced apoptosis as compared

with parental Vero cells based on DNA fragmentation, cytolysis, and nuclear and cellular morphological changes (Figs. 2 and 3). Furthermore, signaling events associated with the induction of apoptosis, such as increases in caspase-3 and -9-like activities, release of cytochrome *c* from mitochondria, and PARP cleavage, occur to a lesser extent in BER-40 cells than in Vero cells, and some of events were even undetectable in BER 40 cells under the conditions tested (Figs. 4 and 5). Furthermore, intracellular biochemical changes associated with apoptosis, such as depletion of glutathione and increase in free Zn²⁺ level, proceed with more delayed time schedule in BER-40 cells than in Vero cells. Since no significant differences in the sensitivity to ricin-mediated protein synthesis inhibition were observed between these cell lines, the results clearly indicate that additional factors or processes are involved in ricin-induced apoptosis apart from those required for the inhibition of protein synthesis. Probably such factors or processes in BER-40 cells may be altered from those in Vero cells. BER-40 cells are also resistant to apoptosis induced by other toxins with different intoxication mechanisms, such as diphtheria toxin, modeccin, and anisomycin. Thus, it seems likely that BER-40 cells have acquired an apoptosis-resistance phenotype regardless of the apoptotic stimuli.

The lack of release of cytochrome *c* from mitochondria in ricin-treated BER-40 cells suggests the possibility that mitochondria in BER-40 cells may be somehow altered. Mitochondria are organelles well known to play a key role in apoptotic signaling (30). We have compared the expression levels of Bcl-2, a regulatory protein involved in the release of cytochrome *c*, in Vero and BER-40 cells by Western blotting. However, no significant differences in the levels of Bcl-2 between Vero and BER-40 cells were observed (Fig. 6). In addition, vital staining of mitochondria with rhodamine 123 showed no differences in the number and structure of mitochondria between Vero and BER-40 cells (data not shown). Therefore, these results suggest that relatively early apoptotic signaling events prior to those that lead to the release of cytochrome *c* may be altered in BER-40 cells, although we can not rule out the possibility that mitochondria-related factors such as Bax and Bcl-x_l, or the phosphorylation/dephosphorylation-related regulation of Bcl-2 function are involved in the apoptosis resistance phenotype in BER-40 cells. Further studies are required to clarify this point.

Although the relationship between BFA-resistance and resistance to toxin-mediated apoptosis in BER-40 cells is still an open question, it is most likely that an alteration in the Golgi region or in Golgi related factors in BER-40 cells may be responsible for the resistance to the induction of apoptosis. One possible candidate is β -COP, but a previous study involving Western blot analysis of total cellular proteins showed that there are no significant differences in the amount or the apparent mobility of the β -COP protein in SDS-PAGE between Vero and BER-40 cells (16). In addition to β -COP, it has been reported that another molecular target of BFA is ADP-ribosylation factor (40). Immunoblot analysis using anti-mouse ARF antibody revealed that no difference in the expression level of ARF between Vero and BEF-40 cells (data not shown). Another possibility is an alteration in the Golgi membrane in BER-40 cells, which may be also confer to BFA-resistance. Regarding this point, our previous study has shown that a water-soluble, mem-

TABLE I. Cytotoxicity of BFA and various anticancer agents in Vero and BER-40 cells.

Drug	IC ₅₀ (nM)*	
	Vero	BER-40
BFA	63.6	2,607.1
Adriamycin	1,700.0	2,000.0
Mitomycin C	14.4	15.8
Vinbrastin	6.5	7.7
Etoposide	160.1	162.1

*IC₅₀, 50% colony formation inhibitory concentration.

brane-permeable ceramide analog, C₆ ceramide, partially restores BFA sensitivity in BER-40 cells based on four distinct effects of BFA; *i.e.* the cytotoxicity of BFA, protection against ricin cytotoxicity by BFA, inhibition of bulk protein secretion by BFA, and the BFA-induced dissociation of β-COP from the Golgi apparatus (41). Since exogenously added ceramide is known to accumulate specifically in the Golgi complex, accumulated C₆ ceramide may affect the physical properties of the Golgi membranes in BER-40 cells to render this mutant cell line susceptible to BFA action. Unfortunately, the effective concentration of C₆ ceramide itself is cytotoxic to BER-40 cells after prolonged incubation (longer than 8 h); thus we could not ascertain whether C₆ ceramide can reverse the resistance of BEF-40 cells to ricin-induced apoptosis.

On the other hand, Mancini *et al.* have recently reported that caspase-2 is localized at the Golgi complex where it cleaves golgin-160, a Golgi-localized macromolecule substrate for caspase-2, during apoptosis (42). Based on these findings, they proposed that the Golgi complex is also an important organelle that senses and transduces apoptotic signals through caspase-2. Thus one can speculate that mutational alterations in the Golgi region, including the Golgi membrane in BER-40 cells, may be deeply involved in the resistance to apoptosis. Perhaps a certain apoptotic signal is transferred from the Golgi complex to the mitochondria, which in turn leads to later apoptotic events such as cytochrome *c* release and the subsequent caspase activation cascade.

In conclusion, our results suggest that one of the phenotypes of BER-40 cells is resistance to apoptosis induced by ricin and other toxins, and that a mutation in the Golgi region is most likely responsible for this phenotype. Further studies of the relationship between the BFA-resistance mechanism and resistance to ricin-induced apoptosis may provide new insights into the mode of action of BFA as well as the mechanism of ricin-induced apoptosis.

REFERENCES

- Middlebrook, J.L. and Dorland, R.B. (1984) Bacterial toxins: cellular mechanisms of action. *Microbiol. Rev.* **48**, 199–221
- Goldstein, J.L., Brown, M.S., Anderson, R.G., Russel, D.W., and Schneider, W.J. (1985) Receptor-mediated endocytosis: concepts emerging from the LDL receptor system. *Annu. Rev. Cell Biol.* **1**, 1–39
- Sandvig, K., Olsnes, S., Brown, J.E., Petersen, O.W., and van Deurs, B. (1989) Endocytosis from coated pits of Shiga toxin: A glycolipid-binding protein in from *Shigella dysenteriae* 1. *J. Cell Biol.* **108**, 1331–1343
- van Deurs, B., Tonnessen, T.I., Petersen, O.W., Sandvig, K., and Olsnes, S. (1986) Routing of internalized ricin and ricin conjugates to the Golgi complex. *J. Cell Biol.* **102**, 37–47
- Van Deurs, B., Sandvig, K., Petersen, O.W., Olsnes, S., Simons, K., and Griffiths, G. (1988) Estimation of the amount of internalized ricin that reaches the trans-Golgi network. *J. Cell Biol.* **106**, 253–267
- Youle, R.J. and Colombatti, M. (1987) Hybridoma cells containing intracellular anti-ricin antibodies show ricin meets secretory antibody before entering the cytosol. *J. Biol. Chem.* **262**, 4676–4682
- Dunphy, W.G. and Rothman, J.E. (1985) Compartmental organization of the Golgi stack. *Cell* **42**, 13–21
- Mellman, I. and Simons, K. (1992) The Golgi complex: in vitro veritas? *Cell* **68**, 829–840
- Misumi, Y., Miki, A., Takatsuki, A., Tamura, G., and Ikehara, Y. (1986) Novel blockade by brefeldin A of intracellular transport of secretory proteins in cultured rat hepatocytes. *J. Biol. Chem.* **261**, 11398–11403
- Oda, K., Hirose, S., Takami, N., Misumi, A., Takatsuki, A., and Ikehara, Y. (1987) Brefeldin A arrests the intracellular transport of a precursor of complement C3 before its conversion site in rat hepatocytes. *FEBS Lett.* **214**, 135–138
- Fujiwara, T., Oda, K., Yokota, S., Takatsuki, A., and Ikehara, Y. (1988) Brefeldin A causes disassembly of the Golgi complex and accumulation of secretory proteins in the endoplasmic reticulum. *J. Biol. Chem.* **263**, 18545–18552
- Lippincott-Schwartz, J., Yuan, L.C., Bonifacino, J.S., and Klausner, R.D. (1989) Rapid redistribution of Golgi proteins into the ER in cells treated with brefeldin A: Evidence for membrane cycling from Golgi to ER. *Cell* **56**, 801–813
- Doms, R.W., Russ, G., and Yewdell, J.W. (1989) Brefeldin A redistributes resident and itinerant Golgi proteins to the endoplasmic reticulum. *J. Cell Biol.* **109**, 61–72
- Yoshida, T., Chen, C.H., Zhang, M., and Wu, H.C. (1990) Increased cytotoxicity of ricin in a putative Golgi-defective mutant of chinese hamster ovary cell. *Exp. Cell Res.* **190**, 11–16
- Yoshida, T., Chen, C.H., Zhang, M., and Wu, H.C. (1991) Disruption of the Golgi apparatus by brefeldin A inhibits the cytotoxicity of ricin, modeccin, and *Pseudomonas* toxin. *Exp. Cell Res.* **192**, 389–395
- Chen, C.H., Kuwazuru, Y., Yoshida, T., Nambiar, M.P., and Wu, H.C. (1992) Isolation and characterization of a brefeldin A-resistant mutant of monkey kidney Vero cells. *Exp. Cell Res.* **203**, 321–328
- Hunziker, W., Whitney, J.A., and Mellman, I. (1991) Selective inhibition of transcytosis by brefeldin A in MDCK cells. *Cell* **67**, 617–627
- Hunziker, W., Whitney, J.A., and Mellman, I. (1991) Selective inhibition of transcytosis by brefeldin A in MDCK cells. *Cell* **67**, 617–627
- Low, S.H., Wong, S.H., Tang, B.L., Tan, P., Subramaniam, V.H., and Hong, W. (1991) Inhibition by brefeldin A of protein secretion from the apical cell surface of Madin-Darby canine kidney cells. *J. Biol. Chem.* **266**, 17729–17732
- Sandvig, K., Prydz, K., Hansen, S.H., and van Deurs, B. (1991) Ricin transport in brefeldin A-treated cells: correlation between Golgi structure and toxic effect. *J. Cell Biol.* **115**, 971–981
- Sandvig, K. and van Deurs, B. (1992) Toxin-induced cell lysis: Protection by 3-methyladenine and cycloheximide. *Exp. Cell Res.* **200**, 253–262
- Oda, T., Komatsu, N., and Muramatsu, T. (1997) Cell lysis induced by ricin D and ricin E in various cell lines. *Biosci. Biotechnol. Biochem.* **61**, 291–297
- Oda, T., Komatsu, N., and Muramatsu, T. (1998) Diisopropylfluorophosphate (DFP) inhibits ricin-induced apoptosis of MDCK cells. *Biosci. Biotechnol. Biochem.* **62**, 325–333
- Mise, T., Funatsu, G., Ishiguro, M., and Funatsu, M. (1977) Isolation and characterization of ricin E from castor beans. *Agric. Biol. Chem.* **41**, 2041–2046
- Oda, T. and Wu, H.C. (1993) Cerulenin inhibits the cytotoxicity of ricin, modeccin, *Pseudomonas* toxin, and diphtheria toxin in brefeldin A-resistant cell lines. *J. Biol. Chem.* **268**, 12596–12602
- Komatsu, N., Nakagawa, M., Oda, T., and Muramatsu, T. (2000) Depletion of intracellular NAD⁺ and ATP levels during ricin-induced apoptosis through the specific ribosomal inactivation results in the cytolysis of U937 cells. *J. Biochem.* **128**, 463–470
- Anderson, M.E. (1985) Determination of glutathione and glutathione disulfide in biological samples. *Methods Enzymol.* **113**, 548–555
- Oda, T., Iwaoka, J., Komatsu, N., and Muramatsu, T. (1999) Involvement of N-acetylcysteine-sensitive pathways in ricin-induced apoptotic cell death in U937 cells. *Biosci. Biotechnol. Biochem.* **63**, 341–348
- Komatsu, N., Oda, T., and Muramatsu, T. (1998) Involvement of both caspase-like proteases and serine proteases in apoptotic cell death induced by ricin, modeccin, diphtheria toxin, and *Pseudomonas* toxin. *J. Biochem.* **124**, 1038–1044

30. Adrain, C. and Martin, S.J. (2001) The mitochondrial apoptosome: a killer unleashed by the cytochrome seas. *TIBS Rev.* **26**, 390–397
31. Reed, J.C., Jurgenmeier, J.M., and Matsuyama, S. (1998) Bcl-2 family proteins and mitochondria. *Biochim. Biophys. Acta* **1366**, 127–137
32. Yang, J., Liu, X., Bhalla, K., Kim, C.N., Ibrado, A.M., Cai, J., Peng, T.I., Jones, D.P., and Wang, X. (1997) Prevention of apoptosis by Bcl-2: release of cytochrome *c* from mitochondria blocked. *Science* **275**, 1129–1132
33. Reed, J.C. (1994) Bcl-2 and the regulation of programmed cell death. *J. Cell Biol.* **124**, 1–6
34. Tamura, T., Sadakata, N., Oda, T., and Muramatsu, T. (2002) Role of zinc ions in ricin-induced apoptosis in U937 cells. *Toxicol. Lett.* **132**, 141–151
35. Orci, L., Tagaya, M., Amherdt, M., Perrelet, A., Donaldson, J.G., Lippincott-Schwartz, J., Klausner, R.D., and Rothman, J. E. (1991) Brefeldin A, a drug that blocks secretion, prevents the assembly of non-clathrin-coated buds on Golgi cisternae. *Cell* **64**, 1183–1195
36. Lippincott-Schwartz, J., Yuan, L., Tipper, C., Amherdt, M., Orci, L., and Klausner, R.D. (1991) Brefeldin A's effects on endosomes, lysosomes, and the TGN suggest a general mechanism for regulating organelle structure and membrane traffic. *Cell* **67**, 601–616
37. Hunziker, W., Whitney, J.A., and Mellman, I. (1991) Selective inhibition of transcytosis by brefeldin A in MDCK cells. *Cell* **67**, 617–627
38. Ktistakis, N.T., Roth, M.G., and Bloom, G.S. (1991) PtK1 cells contain a nondiffusible, dominant factor that makes the Golgi apparatus resistant to brefeldin A. *J. Cell Biol.* **113**, 1009–1023
39. Donaldson, J.G., Lippincott-Schwartz, J., Bloom, G.S., Kreis, T.E., and Klausner, R.D. (1991) Guanine nucleotide modulate the effects of brefeldin A in semipermeable cells: regulation of the association of a 110-kD peripheral membrane protein with the Golgi apparatus. *J. Cell Biol.* **112**, 579–588
40. Donaldson, J.G., Cassel, D., Kahn, R.A., and Klausner, R.D. (1992) ADP-ribosylation factor, a small GTP-binding protein, is required for binding of the coatomer protein β -COP to Golgi membranes. *Proc. Natl. Acad. Sci. USA* **89**, 6408–6412
41. Oda, T. and Chen, C.H., and Wu, H.C. (1995) Ceramide reverses brefeldin A (BFA) resistance in BFA-resistant cell lines. *J. Biol. Chem.* **270**, 4088–4092
42. Mancini, M., Machamer, C.E., Roy, S., Nicholson, D.W., Thornberry, N.A., Casciola-Rosen, L.A., and Rosen, A. (2000) Caspase-2 is localized at the Golgi complex and cleaves golgin-160 during apoptosis. *J. Cell Biol.* **149**, 603–612